

Catalyst Leaching as an Efficient Tool for Constructing New Catalytic Reactions: Application to the Synthesis of Cyclic Vinyl Sulfides and Vinyl Selenides

Valentine P. Ananikov,^{*,[a]} Konstantin A. Gayduk,^[a] Irina P. Beletskaya,^{*,[b]} Victor N. Khrustalev,^[c] and Mikhail Yu. Antipin^[c]

Keywords: Homogeneous catalysis / Leaching / Nickel / Palladium / Nanoparticles

Catalyst leaching from Pd and Ni particles stabilized by organic sulfur and selenium ligands occurs in solution in the presence of phosphanes. This process has been monitored in real time by 1D and 2D NMR spectroscopy and the nature of the metal species established. This catalyst leaching is shown to be a powerful tool for generating new catalytic activity from species formed in situ where the parent bulk particles

are inactive. The catalytic system developed has been successfully implemented in a novel synthetic procedure that provides new types of cyclic sulfur and selenium compounds in high yields through the reaction between alkynes and dichalcogenides.

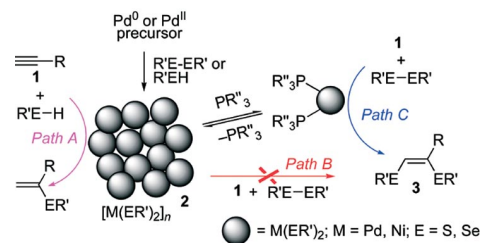
(© Wiley-VCH Verlag GmbH & Co. KGaA, 69451 Weinheim, Germany, 2009)

1. Introduction

The development of nanoparticle catalysts is an area of tremendous growth with several well-established possibilities and promises for the chemical industry. Recent studies have emphasized that the leaching of metal atoms from nanoparticles is a key problem in understanding the mechanistic picture of catalytic cycles involving nanoparticles. The leaching of metal species, and the relationship between the resulting homogeneous and heterogeneous pathways, are recognized as the most important factors which determine the efficiency, stability, and practical usability of catalytic systems.^[1]

Recently, we have found that nanosized Pd and Ni particles stabilized with organic sulfur or selenium ligands $[M(ER')_2]_n$ are excellent catalysts for the regioselective addition of S–H and Se–H bonds to terminal alkynes such as **1** (Scheme 1, path A).^[2] These nanoparticles (**2**) were synthesized from M^0 or M^{II} precursors in a self-organized manner (no catalyst support was required for the synthesis and operation of the catalyst). The catalyst was found to be

inactive in S–S or Se–Se bond addition to alkynes (path B).^[2,3] Surprisingly, catalyst leaching facilitated by phosphane ligands initiated this chemical transformation, which furnished product **3** via path C with excellent stereoselectivity and yields. The presence of a phosphane ligand was also found to be important to facilitate C–E reductive elimination as a final product-releasing step in path C instead of C–H bond formation as a final step in path A.



Scheme 1. Catalytic E–H and E–E bond addition to alkynes under heterogeneous and homogeneous conditions.

Herein we utilize a catalyst leaching process to solve an important problem, namely the synthesis of cyclic vinyl chalcogenides from readily available alkynes and dichalcogenides.^[4] In this study, the active form of the catalyst was prepared in situ from a convenient Pd^0 source $[Pd_2(dba)_3]$ and the desired nature of the metal species was maintained by adjusting the type and relative amount of phosphane ligand present. In addition, we have developed an efficient NMR methodology to distinguish between mono- and polynuclear metal species in situ. It should be noted that the present study highlights an unusual application of catalyst leaching towards the development of “smart” multipurpose catalytic systems.

[a] Zelinsky Institute of Organic Chemistry, Russian Academy of Sciences
Leninsky Prospect 47, Moscow 119991, Russia
Fax: +7-499-135-5328
E-mail: val@ioc.ac.ru

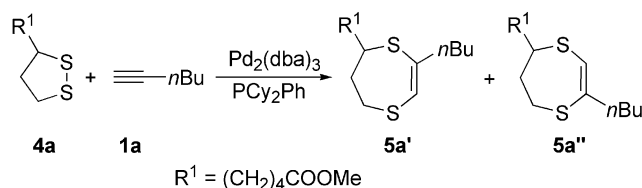
[b] Chemistry Department, Lomonosov Moscow State University
Vorob'evy gory, Moscow 119899, Russia
Fax: +7-495-939-3618
E-mail: beletska@org.chem.msu.ru

[c] Nesmeyanov Institute of Organoelement Compounds, Russian Academy of Sciences,
Vavilova str. 28, Moscow 119991, Russia

Supporting information for this article is available on the WWW under <http://www.eurjic.org> or from the author.

2. Results and Discussion

Several ligands were tested in the model reaction between 1-hexyne (**1a**) and **4a** to optimize the performance of the catalytic reaction (Scheme 2). Disulfide **4a** was chosen as a model compound because it proved to be the most stable of the compounds studied towards polymerization (additional advantages of **4a** for mechanistic studies will be discussed later).



Scheme 2. Pd-catalyzed addition of **4a** to **1a** (140 °C, 8 h).

The yields observed with the studied ligands are given in Table 1. The ligands PCy₃ and DPPE performed poorly in the catalytic reaction, giving product yields of only around 1% after 8 h at 140 °C (entries 1, 2). Better results were obtained with PPh₃ and PCyPh₂ (19%, entries 3, 4) as well as DPPM, which gave 35% of **5a** (entry 5). More promising results were observed with several other phosphane ligands (45–53%, entries 6–8) and the phosphite ligand P(O*i*Pr)₃ (65%, entry 9). The best results, however, were achieved with PCy₂Ph, which gave complete conversion of **4a** under these conditions (entry 10).

Table 1. Various ligands used in the Pd-catalyzed addition of **4a** to **1a**.^[a]

Entry	Ligand	% Yield ^[b]
1	PCy ₃	≈1
2	DPPE	≈1
3	PPh ₃	19
4	PCyPh ₂	19
5	DPPM	35
6	PMe ₂ Ph	45
7	P(allyl) ₂ Ph	47
8	PCy(<i>o</i> -MePh) ₂	53
9	P(O <i>i</i> Pr) ₃	65
10	PCy ₂ Ph	99

[a] 1 mmol of **4a**, 1 mmol of **1a**, 1.5 mol-% of Pd₂(dba)₃, 30 mol-% of ligand, 0.6 mL of toluene, 140 °C, 8 h. [b] Yield of **5a'**+**5a''** determined by NMR spectroscopy and calculated based on initial amount of **4a**.

As can be seen from Table 1, the steric effect of the phosphane ligand increases the performance of the catalytic system [PCy(*o*-MeC₆H₄)₂ (53%) > PCyPh₂ (19%) and PCy₂Ph (99%) > PMe₂Ph (45%)]. However, the overall ligand effect is rather complicated and depends on both the electronic and steric properties of the phosphane ligands, as exemplified by the series of PCy_xPh_y ligands [PCy₂Ph (99%) > PCyPh₂ (19%), PPh₃ (19%) > PCy₃ (1%)]. Thus, ligand screening revealed that the high performance catalytic reaction of interest is possible with Pd species and PCy₂Ph.^[5,6] The overall NMR yield of product **5a** was 99% (89% yield of isolated product).

Surprisingly, we observed an unexpected influence of the ligand amount on the performance of the catalyst in the studied catalytic reaction. For the purpose of this study the same model reaction as described above (**1a** + **4a**, 140 °C, toluene) was utilized, except it was carried out for a shorter time (2 h) to ensure correct comparison of catalytic system performance (Table 2). We found that the yield of **5a** increased upon increasing the concentration of the ligand in solution, and even a 20-fold excess of the ligand did not suppress the catalytic activity. The highest amount of ligand led to the best performance under these conditions (Table 2).

Table 2. Ligand effect on Pd-catalyzed addition of **4a** to **1a**.^[a,b]

Entry	Ligand (amount, mol-%)	L/Pd ratio	% Yield ^[c]
1	PCy ₂ Ph (6)	2	15
2	PCy ₂ Ph (15)	5	40
3	PCy ₂ Ph (30)	10	67
4	PCy ₂ Ph (45)	15	84
5	PCy ₂ Ph (60)	20	94

[a] 1 mmol of **4a**, 1 mmol of **1a**, 1.5 mol-% of Pd₂(dba)₃, 0.6 mL of toluene, 140 °C, 2 h. [b] A control experiment was carried out to confirm the catalytic nature of the system – no reaction between the alkyne and disulfide occurred in the absence of palladium. [c] Yield of **5a'**+**5a''** determined by NMR spectroscopy and calculated based on the initial amount of **4a**.

For economic and environmental reasons it is desirable to use as small an amount of ligand as possible. However, decreasing the amount of ligand in this system would increase the reaction time significantly and facilitate side-reactions. We therefore chose the catalytic system with 30 mol-% of ligand (L/Pd = 10:1), which provides a reasonable compromise between these opposing factors.

This result is in sharp contrast to other known catalytic systems for E–E bond addition.^[7] For example, Sn–Sn bond addition to alkynes shows the expected ligand dependence, namely that an excess of ligand quickly suppresses the catalytic activity (Figure 1). Therefore, by analyzing the influence of the L/Pd ratio on the reaction yield, we can distinguish between a purely homogeneous system and a catalyst leaching issue and can assume that, in the case of

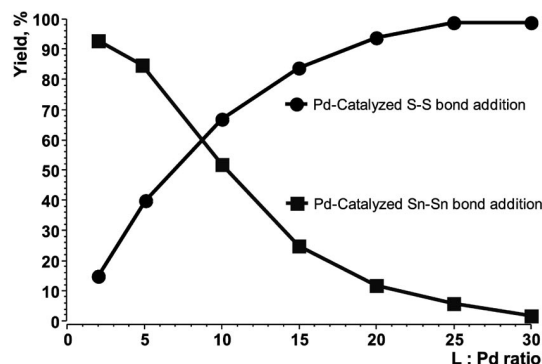
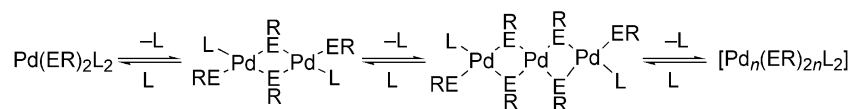


Figure 1. A plot of product yield vs. L/Pd ratio in S–S and Sn–Sn bond additions to alkynes.



Scheme 3. Formation of polynuclear species.

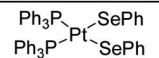
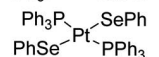
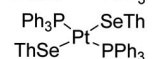
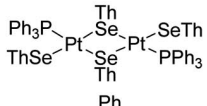
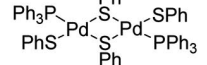
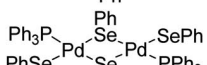
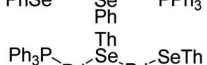
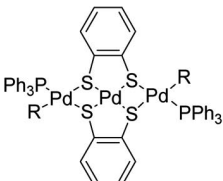
catalyst leaching initiated by the ligand, the larger L/Pd ratio should lead to a higher concentration of active species in solution.

A mechanistic study was clearly required to understand the nature of this catalytic reaction and reveal the key properties of the system. Chalcogenide complexes of Pd are known to undergo phosphane ligand dissociation followed by formation of polynuclear species (Scheme 3). Mononuclear complexes of Pd are unstable and have been isolated in only a few cases, whereas di- and polynuclear complexes are readily formed. One important drawback of this polymerization originates from the low solubility of polymeric species (an insoluble dark brown precipitate was very often formed in Pd chalcogenide systems), which means that the transition metal complex is no longer present in solution and the catalytic reaction stops. This is one of the common symptoms of catalyst poisoning by sulfur and selenium species.^[3]

A series of excellent studies on this subject has been carried out recently by Laitinen et al.,^[9,10,13,15] and a unique trinuclear Pd complex has been isolated by Tokitoh et al.^[14] Representative examples of chalcogenide complexes of Pd and their Pt analogs are shown in Table 3. Unfortunately, the mechanistic nature of these transformations is rather difficult to rationalize due to: i) complicated structural changes, ii) the presence of a number of different species, and iii) the lack of an appropriate analytic tool for in situ monitoring. This lack of a suitable analytic tool is a question of particular importance. ³¹P NMR spectroscopy could be such a tool, but ³¹P chemical shifts are surprisingly rather insensitive to structural changes in chalcogenide species (Table 3). For example, a geometry change from *cis* to *trans* (entries 1 and 2, Table 3), the nature of the organic group (entries 2 and 3, Table 3), mono- or dinuclear complexes (entries 3 and 4, Table 3), all of which are significant structural changes, result in very small differences in the ³¹P NMR chemical shifts of around 19–21 ppm. Similarly, no significant changes in ³¹P NMR spectra were noted for the dinuclear Pd complexes when changing the chalcogen from S to Se (entries 5 and 6, Table 3) or organic group attached to the chalcogen (entries 6 and 7, Table 3). Tri- and polynuclear species have nearly the same chemical shifts as dinuclear complexes with sulfur and selenium ligands, with a difference in ³¹P NMR chemical shifts of less than 2 ppm (cf. entries 5–9, Table 3).

The sensitivity of ³¹P NMR chemical shifts to solvent, temperature, and concentration effects is around 1–5 ppm,^[16] therefore it is very difficult, if not impossible, to distinguish metal species in solution by ³¹P NMR spectroscopy alone. The unambiguous interpretation of NMR spectroscopic data currently requires the corresponding X-

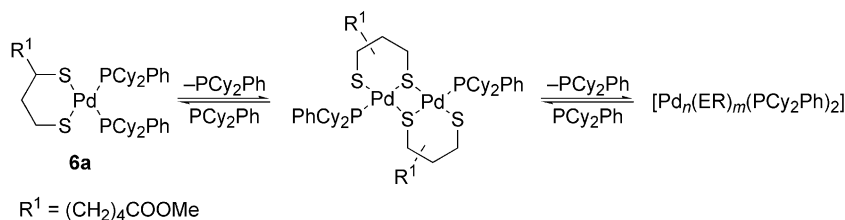
Table 3. Structural and spectral properties of mono-, di-, and polynuclear complexes of Pd and Pt (Th = 2-thienyl).

Entry	Complex	³¹ P NMR (δ, ppm)	Crystal structure
1		18.7 ^[8] 19.1 ^[9]	[8,9]
2		20.8 ^[9]	[9]
3		21.5 ^[10]	[10]
4		20.4 ^[10]	[10]
5		30.4 ^[11]	[12]
6		27.9 ^[13]	[13]
7		29.3 ^[10]	[10]
8		28.5 ^[14]	[14]
9	[Pd _n (SPh) _m (PPh ₃) ₂] <i>n</i> > 2	29.7–30.5 ^[11]	–

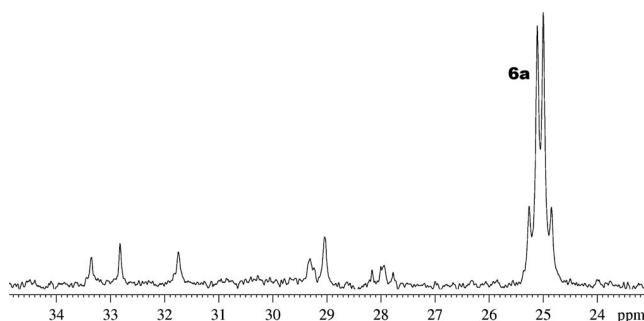
ray analysis to be performed (Table 3). Unfortunately, X-ray analysis can be carried out only in the case of stable complexes, whereas reactive intermediate species, which are generally not isolated, are of most interest for mechanistic studies.

In order to overcome these difficulties we developed a special approach which takes advantage of the unsymmetrical nature of the cyclic dichalcogenide **4a**. In this case, the mononuclear Pd complex gives two doublets in the ³¹P NMR spectrum due to ²J_{P,P} spin-spin coupling, while polymeric species give singlets since ⁿJ_{P,P} coupling constants with *n* ≥ 4 are rather small (Scheme 4).

An sample ³¹P NMR spectrum is shown in Figure 2. Complex **6a** can easily be identified at δ = 25.2 (d, J_{P,P} = 30.7 Hz) and 24.9 ppm (d, J_{P,P} = 30.7 Hz). The remaining signals in the ³¹P spectrum at δ = 27–34 ppm are singlets and correspond to polynuclear species. Note that formation of several isomeric polynuclear complexes is possible due to different orientations of the R¹ group (see Scheme 4). The

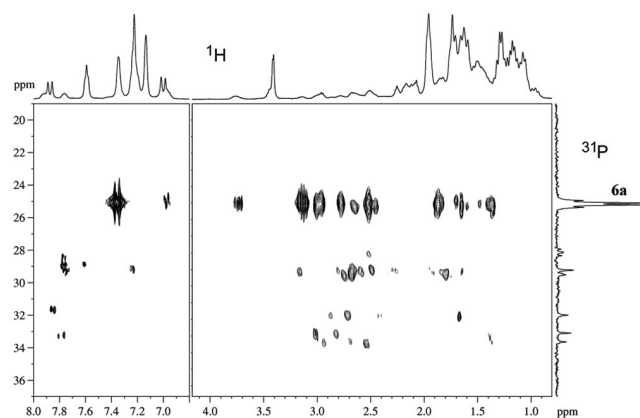
Scheme 4. Polymerization of complex **6a**.

other signals detected in the ^{31}P spectrum at $\delta = 2.5$, 42.3, and 58.9 ppm correspond to PCy_2Ph , $\text{O}=\text{PCy}_2\text{Ph}$, and $\text{S}=\text{PCy}_2\text{Ph}$. For a discussion of a possible mechanism for the formation of $\text{S}=\text{PCy}_2\text{Ph}$ see ref.^[17]

Figure 2. $^{31}\text{P}\{^1\text{H}\}$ NMR spectrum of the $\text{Pd}^0/\text{PCy}_2\text{Ph} + \mathbf{4a}$ reaction mixture.

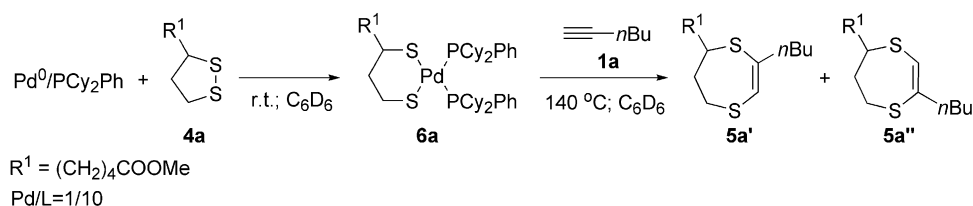
Unambiguous confirmation that the observed ^{31}P NMR signals belong to transition metal complexes formed from $\text{Pd}/\text{PCy}_2\text{Ph}$ and **4a** was obtained from the 2D ^1H - ^{31}P HMQC spectrum (Figure 3). This two-dimensional correlation allows all groups in the metal complexes to be identified: correlation with the proton chemical shifts at $\delta = 1.0$ – 2.0 ppm confirms the presence of a Cy group, those at $\delta = 2.2$ – 4.0 ppm the presence of the cyclic disulfide part, and those at $\delta = 6.9$ – 7.5 ppm the presence of a Ph group. Taking into account that a ^1H - ^{31}P HMQC experiment is inverse detected, and therefore very sensitive (approx. 15 min on routine hardware), we consider it to be a very convenient approach to dealing with this complicated mixture of complexes (a detailed description of the NMR experiment is provided in the Experimental Section). The use of the unsymmetrical cyclic dithiolene **4a** therefore proved to be of great importance for the mechanistic study since it allowed us to identify mono- and polynuclear species simply by inspecting the multiplicity of the signals in ^{31}P NMR spectrum, thus avoiding the need to analyse non-characteristic chemical shift values. The mechanistic study has there-

fore shown that oxidative addition of **4a** to Pd^0 leads to complex **6a**, which was detected in situ by 2D NMR spectroscopy (Figure 3). The NMR study also revealed that **6a** readily polymerizes to form soluble $[\text{Pd}_n(\text{S}\cap\text{S})_n(\text{PCy}_2\text{Ph})_2]$ species. The role of the excess ligand is to suppress this polymerization and maintain the active form of the catalyst – without an excess of the phosphane ligand, only the insoluble metal particles **2** are formed (see Scheme 1) and the catalytic reaction does not take place.

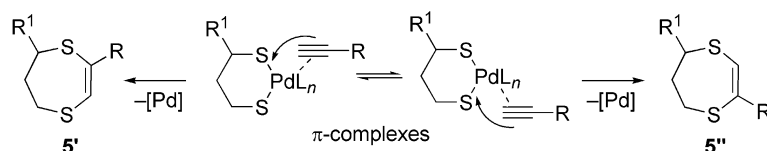
Figure 3. Two-dimensional ^1H - ^{31}P HMQC spectrum of the reaction mixture.

To investigate the next steps of the catalytic reaction we carried out a series of stoichiometric reactions. The first stage – oxidative addition of **4a** to Pd^0 – was studied by ^1H and ^{31}P NMR monitoring in an NMR tube in C_6D_6 solution (Scheme 5). The formation of complex **6a** (40% yield) was observed at room temperature after 30 min and the nature of the metal complexes was again confirmed by 2D ^1H - ^{31}P HMQC spectroscopy.

The second stage – alkyne coordination and insertion – was studied after addition of **1a** to the NMR tube (Scheme 5). Formation of **5a** was not observed at room temperature, although a 90% yield of **5a** was observed after 3 h at 140 °C.



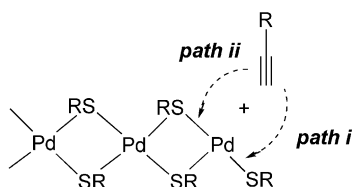
Scheme 5. NMR spectroscopic monitoring of the stoichiometric reactions.



Scheme 6. Alkyne insertion into the M–E bonds of complex 6.

Coordination of the alkyne to compound **6** may lead to two different π complexes and deserves a further note (Scheme 6) as both Pd–S bonds should be available for the alkyne insertion, which means that two products (**5'** and **5''**) should be formed. Indeed, our findings are in excellent agreement with the proposed mechanism since a nearly 1:1 ratio of **5'** and **5''** was observed in the reaction of **4a** with the studied alkyne. If symmetrical cyclic dichalcogenides were involved in the reaction only one product would be expected.

Two different alkyne-insertion pathways are possible for polynuclear derivatives – insertion into the terminal Pd–S bond and insertion into the bridging Pd–S bond (Scheme 7).

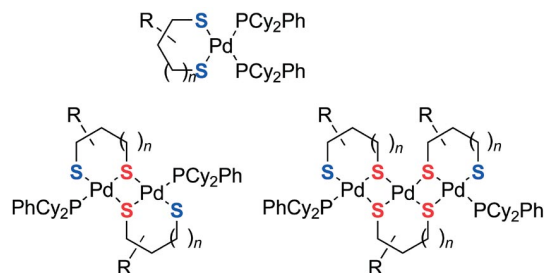


Scheme 7. Alkyne insertion into the terminal (path i) and bridging (path ii) Pd–S bonds.

The relative reactivity of the terminal and bridging Pd–S bonds in dinuclear complexes was recently estimated by theoretical calculations at the B3LYP level^[3b] using a model system, which showed that reaction via pathway (i) encounters only a small activation barrier and is exothermic, whereas reaction via pathway (ii) encounters a much higher barrier and is endothermic. According to these calculations, pathway (i), which involves insertion into the terminal Pd–S bond, is more favorable.

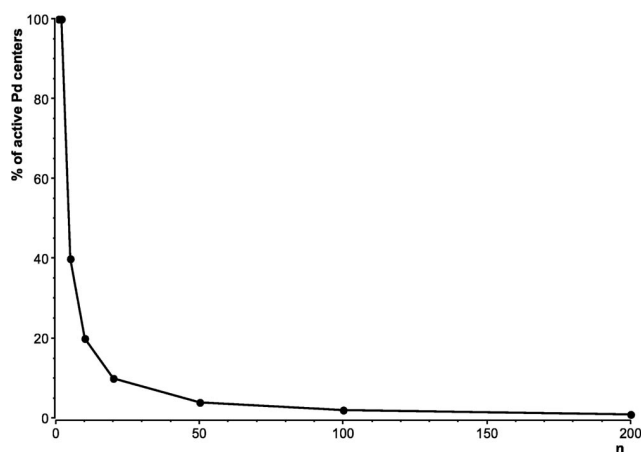
Taking into account the relative reactivity of different sulfur groups discussed above, we can analyze the nature of the catalytic species. In mono- and dinuclear species, all Pd atoms have terminal SR groups attached, therefore the number of catalytically active sites is equal to the number of Pd atoms (Scheme 8). In the trinuclear complex, however, only two (out of three) Pd atoms would demonstrate catalytic activity in the reaction of interest.

The relationship between the percentage of catalytically active Pd atoms in solution versus the total number of Pd atoms in the $[\text{Pd}_n(\text{ER})_m\text{L}_2]$ species is shown in Figure 4. It is evident that the number of catalytically active sites decreases rapidly with increasing length of the polymeric chain. The solubility of Pd complexes is also an important issue which should be taken into account. Several studies have shown that an increase in size of the polynuclear complex results in a decrease of solubility in common organic



Scheme 8. Mono- and polynuclear complexes containing catalytically active terminal Pd–S bonds (blue) and relatively inactive bridging Pd–S bonds (red).

solvents.^[3,8–11] Thus, a small size of the metal species is favorable for both reasons (number of active sites and solubility). We can therefore now rationalize the observed influence of the amount of phosphane ligand on the performance of the catalytic reaction studied (Figure 1) – an excess of phosphane ligand shifts the equilibrium towards the formation of smaller complexes and increases the number of catalytically active sites.

Figure 4. A plot of the estimated percentage of active Pd atoms vs. the total number of Pd atoms (n) in the $[\text{Pd}_n(\text{ER})_m\text{L}_2]$ polymer (see Scheme 8 for examples of $n = 1, 2$, and 3).

We also investigated the catalytic activity of the Ni complex with a view to obtaining a cheaper analog of the Pd catalyst for the studied system. A variety of ligands showed catalytic activity, with different yields, in the Pd-catalyzed reaction discussed above (see Table 1). In contrast to Pd, however, the Ni-catalyzed transformation with $\text{Ni}(\text{acac})_2$ as catalyst precursor proved possible with only a few ligands (Table 4). Most of the studied ligands gave no product (entries 1–6) or only traces of product (entries 7, 8). A notice-

able improvement with the Ni-based catalytic system was observed with P(O*i*Pr)₃ (13%, entry 9) and the best performance was achieved with PMe₂Ph (64%, entry 10).

Table 4. Various ligands used in the Ni-catalyzed addition of **4a** to **1a**.^[a]

Entry	Ligand	% Yield ^[b]
1	PCy ₃	0
2	DPPE	0
3	PPh ₃	0
4	PCyPh ₂	0
5	PCy ₂ Ph	0
6	PCy(<i>o</i> -MePh) ₂	0
7	P(allyl) ₂ Ph	≈1
8	DPPM	3
9	P(O <i>i</i> Pr) ₃	13
10	PMe ₂ Ph	64

[a] 1 mmol of **4a**, 1 mmol of **1a**, 3 mol-% of Ni(acac)₂, 30 mol-% of ligand, 0.3 mL of toluene, 100 °C, 4 h. [b] Yield of **5a'**+**5a''** determined by NMR spectroscopy and calculated based on the initial amount of **4a**.

To estimate the influence of the L/Ni ratio on the performance of the catalytic system the model reaction was carried out for a shorter time of 1 h to prevent several entries having a complete conversion of around 99%. We found that, similar to the Pd system (see Table 2), increasing the L/Ni ratio improved the performance of the catalytic system (Table 5). For practical reasons, we chose the catalytic system with 30 mol-% of ligand (L/Ni = 10:1), which provides a reasonable compromise between the yield of product, the reaction time, and the amount of ligand consumed.

Table 5. Ligand effect on the Ni-catalyzed addition of **4a** to **1a**.^[a]

Entry	Ligand (amount, mol-%)	L/Ni ratio	% Yield ^[b]
1	PMe ₂ Ph (6)	2	1
2	PMe ₂ Ph (15)	5	16
3	PMe ₂ Ph (30)	10	37
4	PMe ₂ Ph (45)	15	56
5	PMe ₂ Ph (60)	20	63

[a] 1 mmol of **4a**, 1 mmol of **1a**, 3 mol-% of Ni(acac)₂, 0.3 mL of toluene, 100 °C, 1 h. [b] Yield of **5a'**+**5a''** determined by NMR spectroscopy and calculated based on the initial amount of **4a**.

Unfortunately, we were unable to repeat the mechanistic NMR spectroscopic study for the Ni complexes due to the very broad lines observed in the ¹H, ¹³C, and ³¹P NMR spectra in the presence of nickel species. This is a well-known phenomenon in spectroscopic studies and is due to the paramagnetic contribution of the metal.^[18] Nevertheless, a similar dependence on the L/Ni ratio is an indication of the formation of polymeric species in the case of Ni catalysts as well.

To obtain clear evidence for catalyst leaching we synthesized the polymeric Ni species **2** from Ni(acac)₂ and **4a**. This species is insoluble in common organic solvents and was isolated as a dark brown solid. Structural characterization of the solid was carried out by scanning electron microscopy (SEM), as shown in Figure 5. According to the SEM study, the solid has a flaky structure and the smallest observed structural units are 100–500 nm in size and 40–90 nm thick. The isolated solid species was successfully utilized as a catalyst for the addition of **4a** to **1a**. The solid phase dissolved in the presence of an excess of phosphane ligand and the resulting soluble Ni species catalyzed formation of the same product (**5a**) with a similar efficiency (65% after 4 h at 100 °C) to the in situ formed catalyst (cf. entry 10, Table 4). A high yield of **5a** (ca. 95%) was observed upon increasing the reaction time. Without phosphane ligand, the polymeric Ni species did not dissolve and did not catalyze the reaction of **4a** and **1a** under similar reaction conditions.

The influence of the phosphane ligand on the catalyst state was also studied for this catalytic system without isolating solid particles. In the first step, the polymeric Ni species **2** was obtained as described above. Heating the reaction mixture containing the insoluble metal species at 100 °C for 4 h resulted in the formation of a trace amount of product **5a** (ca. 5%), as observed by NMR spectroscopy. Subsequent addition of a further amount of ligand (30 mol-% in total) led to dissolution of the insoluble metal species and the yield of product **5a** quickly increased to 56%, 72%, and 90% after heating for 1, 2, and 4 h at 100 °C, respectively. These studies of the reaction mechanism provide a clear demonstration of the leaching effect in the studied catalytic system.

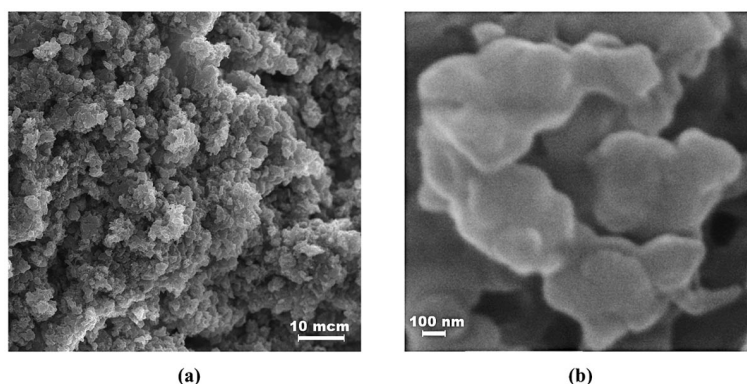
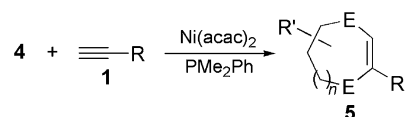


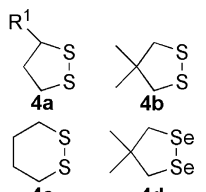
Figure 5. Low- (a) and high-magnification (b) SEM images of the insoluble nickel particles (1000× and 50000×, respectively).

Although the Pd system was a good model for the mechanistic study, we found that the corresponding Ni-catalyzed reaction is superior for synthetic purposes as, since the Pd-catalyzed reaction requires harsh conditions (140 °C, 8 h), it may facilitate the side reaction of cyclic dichalcogenide (**4**) polymerization. Suppressing this polymerization is a rather difficult issue, therefore as the Ni-catalyzed reaction requires much milder reaction conditions (100 °C), it suffers less from the polymerization of **4**.

The scope of the developed synthetic methodology was investigated for various substrates (Table 6). Excellent product yields of 50–91% were obtained and the products were isolated in a pure form. A single product was formed for all symmetric dichalcogenides studied (**4b–4d**), while an equimolar mixture of products was observed with **4a**, in total agreement with the proposed reaction mechanism (see Scheme 6 and discussion therein). Both S–S and Se–Se bonds were found to react with the triple bond of alkynes under the catalytic conditions to give good product yields (Table 6). The lower yields observed for the cyclic diselenide **4d** compared to the isostructural disulfide **4b** are due to the high reactivity of the former and decomposition via side reactions (see entries 2, 5, 8 and entries 10–12, Table 6).

Table 6. Ni-catalyzed addition of alkynes to cyclic disulfides and diselenides.^[a]





R = $n\text{C}_4\text{H}_9$ **1a**
 CH_2OMe **1b**
 CH_2NMe_2 **1c**

$\text{R}' = (\text{CH}_2)_4\text{COOMe}$
 $n = 1, 2$
 $\text{E} = \text{S}, \text{Se}$

Entry	Alkyne	E–E	Product	% Yield ^[b]
1	1a	4a	5a' + 5a''	89
2	1a	4b	5b	86
3	1a	4c	5c	62
4	1b	4a	5d' + 5d''	73
5	1b	4b	5e	91
6	1b	4c	5f	59
7	1c	4a	5g' + 5g''	77
8	1c	4b	5h	72
9	1c	4c	5i	74
10	1a	4d	5j	50
11	1b	4d	5k	64
12	1c	4d	5l	56

[a] 3 mol-% of $\text{Ni}(\text{acac})_2$, 30 mol-% of PMe_2Ph , 0.3–0.5 mL of toluene, 100 °C, 4–10 h. [b] Yield of isolated **5**.

We found that the purity of the cyclic dichalcogenides **4** was one of the key factors in obtaining high product yields, therefore we revised the available synthetic procedures and provide optimized synthetic routes to **4** (see Experimental Section for details). In fact, having a pure compound in hand we were able to determine the first X-ray structure of a five-membered diselenide. Unambiguous confirmation of

the products' structure was obtained by X-ray analysis of **5i** and **5h**.

Compound **4d** is the first example of a structurally characterized 1,2-diselenolane not fused with other cyclic systems and containing a free diselenide group that is not involved in complex formation.^[19]

The crystal structure of **4d** consists of discrete molecules with no short intermolecular contacts. The shortest intermolecular Se...Se distance is 3.989(3) Å, which is larger than the sum of the van der Waals radii of selenium atoms (3.80 Å; see the Supporting Information for geometric parameters).

A perspective view of the molecular structure of **4d** is shown in Figure 6 along with the atomic numbering scheme. The crystal packing of molecules of **4d** involves stacking along the *b* axis (Figure 6). Each molecule of **4d** adopts an envelope conformation with four atoms (Se1, Se2, C3, and C5) forming a plane and one carbon atom (C4) at the envelope flap. The degree of deviation of the ring from planarity can be evaluated from the distance between the C4 atom and the mean plane of the other four ring atoms (0.678 Å). Considering the geometrical dimension of the five-membered ring it can be seen that the two C–Se bond lengths [1.971(2) and 1.966(2) Å] are nearly identical and the same is true for the two C–C bonds [1.528(2) and 1.535(2) Å]. The endo angles at the selenium atoms [91.90(5)° and 91.64(5)°] and at C3 and C5 [111.5(1)° and 110.8(1)°] are also similar to each other. A pseudomirror plane which bisects the Se–Se bond and passes through the C4 atom at the flap can be defined on the basis of these features. Interestingly, **4d** adopts a twist conformation upon coordination to the metal atoms through the Se–Se bridge.^[20]

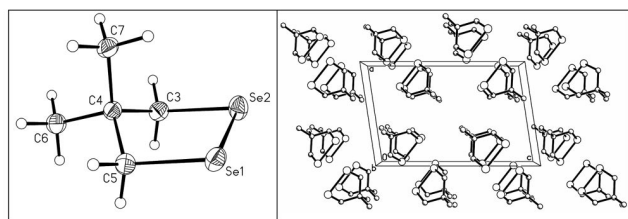


Figure 6. Molecular structure of **4d** and crystal packing.

An interesting correlation between a decrease of the torsion angle around the disulfide bridge and an increase of the S–S bond length has been reported by Bock et al.^[21] It is now well established that the major contribution to the enhanced reactivity of 1,2-dithiolanes arises from the small dihedral angle around the S–S bond associated with the reduced size of the ring and by the resulting unfavorable interaction between the adjacent sulfur lone pairs.^[22] Accordingly, the S–S bond in 1,2-dithiolanes is longer and weaker than that found in open-chain disulfides, whose dihedral angle is close to 90°. Similar geometrical peculiarities are also characteristic for the related compound **4d**, in which the dihedral angle around the diselenide bridge is 0.57(7)° and the Se–Se bond length [2.3580(3) Å] is longer than that in strain-free, open-chain diselenides (2.340 Å). Thus, the

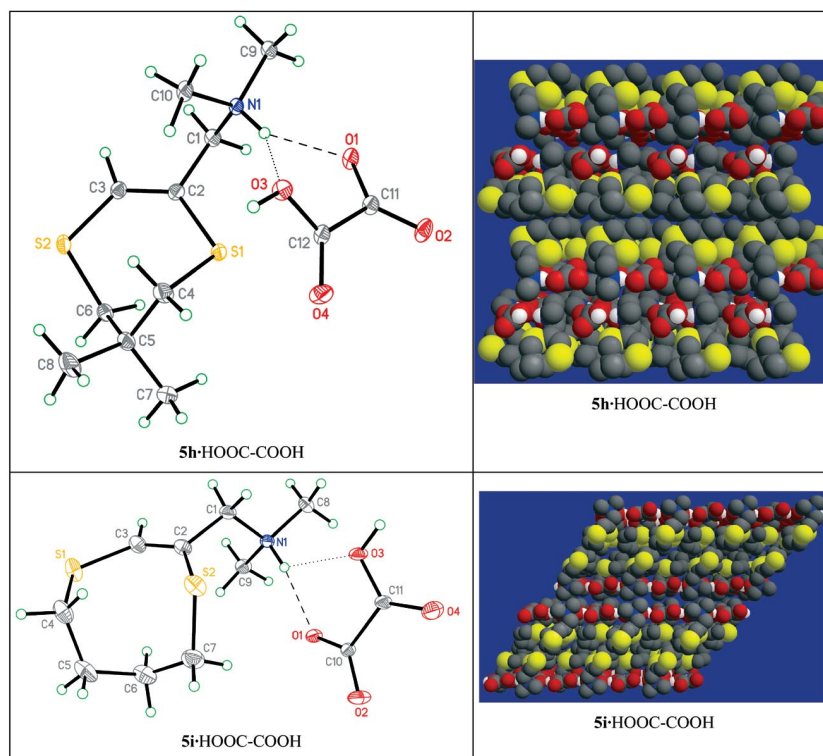


Figure 7. Molecular structures of **5h**-HOOC-COOH and **5i**-HOOC-COOH and the crystal packing.

investigated 1,2-diselenolane **4d** should possess a high reactivity, as confirmed by its chemical properties described herein.

The crystal structures of compounds **5h** and **5i** are shown in Figure 7, along with the atomic numbering schemes (see the Supporting Information for geometric parameters). These compounds were crystallized as salts involving ammonium sulfur-containing $[(RS)HC=C(SR)CH_2NHMe_2]^+$ cations and oxalate $[HOOC-COO]^-$ anions, which form tight ionic pairs due to the bifurcated hydrogen bonds between the amino-H atom of the cation and two oxygen atoms of the anion. It is interesting to note that compounds **5h** and **5i** contain rare structurally characterized seven-membered 6,7-dihydro-5*H*-1,4-dithiepine and eight-membered 5,6,7,8-tetrahydro-1,4-dithiocine rings, respectively, neither of which are fused with other cyclic systems. Whereas only two X-ray structures of two- or three-substituted 6,7-dihydro-5*H*-1,4-dithiepine derivatives are available,^[23] no structures containing a substituted 5,6,7,8-tetrahydro-1,4-dithiocine ring have been reported.

The seven-membered ring in **5h** has a twisted conformation with a planar S1-C2-C3-S2/C5 moiety. The carbon atoms C4 and C6 deviate from the plane containing the other atoms of the ring by -0.895 and $+0.881$ Å, respectively. The dihedral angle between the S1-C2-C3-S2/C5 and C4-C5-C6 planes is 44.9° . The local symmetry is C_2 , with the pseudo twofold axis passing through the middle of the C2-C3 bond and the carbon C5 atom.

The conformation of the eight-membered ring in **5i** is tub-shaped, with three planar C4-S1-C3-C2-S2, C4-C5/

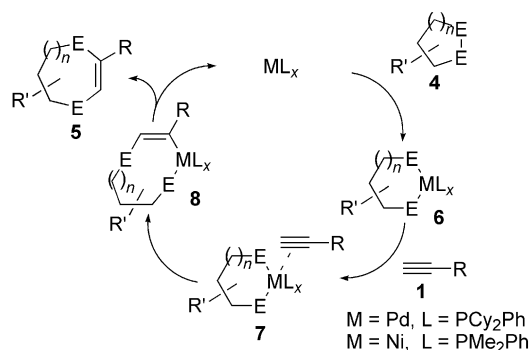
C7-S2 and C5-C6-C7 moieties. The dihedral angles between the C4-S1-C3-C2-S2 and C4-C5/C7-S2 planes and the C5-C6-C7 and C4-C5/C7-S2 planes are 67.9° and 54.9° , respectively. There are no intermolecular S...S contacts shorter than 3.7 Å in the crystals of either compound.

3. Conclusions

According to the study reported herein, the overall catalytic cycle involves the following steps: 1) oxidative addition (**6**); 2) alkyne coordination to form π complex **7**; 3) alkyne insertion into the M-E bond (**8**); and 4) reductive elimination from the phosphane complex **8** to give product **5** and regenerate the metal species (Scheme 9). A series of stoichiometric reactions has been carried out to confirm the proposed mechanism of the catalytic reaction. For clarity reasons only mononuclear metal complexes are shown in Scheme 9, although other metal species may also contribute to product formation with varying degrees of success.

It should be pointed out that the excess of phosphane ligand might be expected to decrease the performance of the catalytic reaction due to coordination to the metal, as shown in Scheme 9, and that the catalyst is totally inactive in the absence of phosphane ligand. Therefore, even if the reaction rate is decreased by the ligand excess, this seems to be the best way of maintaining the catalyst in its active form. We have shown that both types of ligand effect are possible (see also Figure 1).

To summarize, we have developed a novel synthetic procedure to access new types of sulfur and selenium com-



Scheme 9. Plausible mechanism for the catalytic reaction.

pounds (**5**) in high yields and have revealed the origins of the extraordinary properties of the catalytic system. This methodology is likely to be of great interest for synthetic purposes and could also draw further attention to catalyst leaching as a flexible tool for enhancing the catalytic applications of nanoparticles.

The multipurpose catalytic systems studied herein govern different reactions – S–H, Se–H (bulk nanoparticles)^[3] and S–S, Se–Se (leached catalyst) bond additions to alkynes – with high selectivity, in contrast to previous reports, where bulk and leached catalysts were assumed to catalyze the same reaction.

Experimental Section

General Procedures: Unless otherwise noted, all synthetic work was carried out under argon. Pd₂(dba)₃ was prepared according to a published procedure.^[24] Ni(acac)₂ was dried under vacuum (0.1–0.05 Torr, 60 °C, 30 min) before use. Other reagents were obtained from Acros and Lancaster and used as supplied (checked by NMR spectroscopy before use). Solvents were purified according to published methods. The reaction was carried out in PTFE screw-capped tubes or flasks.

All NMR measurements were performed using a three-channel Bruker AVANCE 500 spectrometer operating at 500.1, 202.5, and 125.8 MHz for ¹H, ³¹P, and ¹³C, respectively. The spectra were processed on a Linux workstation using the TOPSPIN software package. All 2D spectra were recorded using an inverse triple-resonance probehead with an active-shielded Z-gradient coil. The ¹H and ¹³C chemical shifts are reported relative to the corresponding solvent signals used as internal reference. Estimated errors in the yields determination by ¹H NMR are less than 2%. The SEM study was carried out with a JEOL JSM-6380 microscope.

Pd-Catalyzed Sn–Sn Addition: This reaction (see Figure 1) was carried out according to the literature method^[25] as follows. Sn₂Me₆ (0.5 mmol), 1-ethynyl-1-cyclohexanol (1.0 mmol), the appropriate amount of PPh₃ (L/Pd ratios of 2:1, 5:1, 10:1, 15:1, 20:1, 25:1, and 30:1 were examined), and 2.5 mol-% of Pd₂(dba)₃ were stirred in 0.3 mL of toluene at 16 h for 85 °C. The yield was measured by ¹H NMR spectroscopy. The *syn*-addition product was formed.

Synthesis of Substrates 4a–4d: Cyclic dithiolanes (**4**) are rather prone to polymerization,^[26] and we found that the polymeric materials were inactive in the catalytic reactions of interest. Moreover, even a small amount of polymer contamination dramatically reduced the performance of the catalytic reaction. Special care should

therefore be taken to prevent polymerization of the substrates (preferably by using freshly synthesized species in the reaction). The compounds should not be exposed to a daylight for a long time, although they can be stored at –17 °C for a short time (1 week).

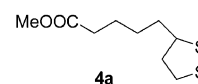
Among the studied compounds, **4c** and **4d** proved especially sensitive to polymerization. We found that monomeric and polymeric species have rather similar NMR chemical shifts and cannot be clearly distinguished spectroscopically.

It proved useful to check the m.p. of **4c** before each synthesis (28–30 °C^[27]), while >100 °C for the corresponding polymer.

Compound **4d** should be used as pure crystals (m.p. 26 °C^[28]) without oil contamination (the polymer seems to be partially oily).

The original synthetic procedures available in the literature were therefore carefully checked and modified to avoid polymerization during preparation and purification of these compounds (references for the original procedures are provided in each case).

Methyl (±)-α-Lipoate^[29] (4a): DL-thioctic acid (10.0 g, 48 mmol) and 100 mL of diethyl ether were placed into a 300-mL glass beaker equipped with a magnetic stir bar and cooled in a water/ice bath. Stirring was continued until a homogeneous yellow solution had formed. A solution of diazomethane in 120 mL of diethyl ether was prepared separately from (9.17 g, 88.9 mmol) of nitrosomethyl urea (distillation of diazomethane was not required).^[30] This solution was slowly added to the solution of DL-thioctic acid and stirred for 15 min. The color of the reaction mixture remained yellow. The solution was then warmed to room temperature whilst stirring and kept at room temperature until evaporation of 1/5 of its volume. The rest of the solvent was then removed in vacuo and the pure product obtained by distillation (89 °C, 0.04 Torr), yield 9.6 g (90%) of yellow oil.

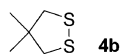


Caution! Due to the potentially hazardous and toxic nature of diazomethane, great care is required during synthesis and all manipulations. See the appropriate safety regulations for detailed information.

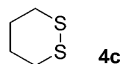
The product was identified based on the published ¹H and ¹³C NMR spectroscopic data.^[31]

4,4-Dimethyl-1,2-dithiolane^[28] (4b): Refined sulfur (1.67 g, 6.5 mmol of S₈), powdered NaOH (3.13 g, 78.3 mmol), and 50 mL of dmf were placed into a 100-mL two-necked flask equipped with a magnetic stir bar (under argon) and 0.71 mL of 100% hydrazine hydrate (14.6 mmol) was added slowly (over 30 min using syringe pump). After nitrogen evolution had ceased a dark-green solution was obtained. The solution was stirred for 6 h at room temperature then a solution of 1,3-dibromo-2,2-dimethylpropane^[32] (6.0 g, 26.1 mmol) in 15 mL of dmf was added slowly (over 30 min using a syringe pump). The temperature of the solution was raised by 10–15 °C and then lowered to room temperature. Stirring was continued for 3 h and the mixture was then left to stand for 12 h at room temperature to give an almost colorless solution and a white solid. The reaction mixture was added to 200 mL of distilled water and extracted three times with 40 mL of dichloromethane. The organic phase was washed twice with 40 mL of 6 M HCl, then with 200 mL of distilled water and dried over Na₂SO₄. The pure product was obtained after chromatography on silica with a hexanes/dichloromethane gradient (9:1→1:1), yield 1.7 g (50%) of yellow oil. The product was identified based on the published ¹H NMR spectro-

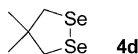
scopic data.^[33] $^{13}\text{C}\{^1\text{H}\}$ NMR (126 MHz, CDCl_3): δ = 51.37, 47.29, 27.06 ppm.



1,2-Dithiane^[26c] (4c): Silica (15:40, 100 g) was placed into a 1-L flask and 50 mL of distilled water was slowly added with rigorous stirring until a uniform suspension had formed. Dichloromethane (500 mL) and a solution of 1,4-butanedithiol (4.89 g, 40 mmol) in 50 mL of dichloromethane were added to this suspension whilst stirring. A solution of Br_2 (7.03 g, 44 mmol) in 40 mL of dichloromethane was slowly added to the stirred suspension to give a colorless solution. The addition of bromine was terminated when the color of the suspension turned light yellow and did not disappear after 10 min of stirring. This reaction mixture was filtered into a flask containing a solution of 12 g of NaOH (300 mmol) in 240 mL of distilled water (whilst stirring). The colorless organic phase was separated, washed three times with 150 mL of distilled water and dried over Na_2SO_4 . The solvent was removed in vacuo and the crude product crystallized from hexanes at -17°C , yield 4.1 g (85%) of a white crystalline solid. The product was identified based on the published ^1H and ^{13}C NMR spectroscopic data.^[27,34]



4,4-Dimethyl-1,2-diselenolane^[28] (4d): Selenium (200 mesh; 4.12 g, 52.2 mmol), powdered NaOH (3.13 g, 78.3 mmol), and 50 mL of dmf were placed into a 100-mL two-necked flask equipped with a magnetic stir bar (under argon) and 0.71 mL of 100% hydrazine hydrate (14.6 mmol) was added slowly (over 30 min using a syringe pump). After nitrogen evolution had ceased a dark brown solution was obtained. This solution was stirred for 6 h at room temperature and then a solution of 1,3-dibromo-2,2-dimethylpropane (6.0 g, 26.1 mmol)^[32] in 15 mL of dmf was added slowly (over 30 min using a syringe pump). The temperature of the solution was raised by 10 – 15°C and then lowered to room temperature. Stirring was continued for 3 h and the mixture was then allowed to stand for 12 h at room temperature. The color of the solution remained unchanged. The reaction mixture was added to 200 mL of distilled water and extracted three times with 40 mL of dichloromethane. The organic phase was washed twice with 40 mL of 6 M HCl, then with 200 mL of distilled water and dried over Na_2SO_4 . The product was purified by chromatography on silica with a hexanes/dichloromethane gradient (9:1→4:1). Further purification was achieved by crystallization from hexanes at -17°C (twice) followed by washing with cold hexanes, yield 3.0 g (50%) of magenta colored crystals. The product was identified based on the published ^1H and ^{13}C NMR spectroscopic data.^[33,35]



2D ^1H - ^{31}P HMQC NMR Experiment: The spectrum was collected with 90° ^1H and ^{31}P pulses of 12.5 and 9.5 μs respectively, a relaxation delay of 2 s, $\Delta = (2^* J_{\text{H,P}})^{-1} = 25$ ms (optimized for coupling constant of 20 Hz), a 0.28-s acquisition time, and spectral windows of 4000 and 20000 Hz for the ^1H (F2) and ^{31}P (F1) dimensions, respectively. Four transients were averaged for each of 256 increments on t_1 . The 1-ms sine-shaped pulse field gradient pulses with the ratio 50.0:30.0:52.3% were followed by a 100- μs recovery delay. The data were zero-filled to a 2048×2048 matrix and pro-

cessed with the QSINE (SSB = 2) window function for both the F2 and F1 dimensions. Linear prediction was applied to enhance the quality of the spectrum.

Stoichiometric Reactions Under NMR Monitoring (Scheme 5): $\text{Pd}_2(\text{dba})_3$ (0.0200 g, 1.93×10^{-5} mol), Cy_2PhP (0.0530 g, 1.93×10^{-4} mol), and methyl (\pm)- α -lipoate (0.0085 g, 3.86×10^{-5} mol) were placed into an NMR tube and dissolved in 0.5 mL of C_6D_6 . The ^1H , $^{13}\text{P}\{^1\text{H}\}$, and 2D ^1H - ^{31}P HMQC spectra of the dark-brown solution were recorded after shaking the tube for 30 min at room temperature. The reaction mixture was then placed into a PTFE-sealed tube equipped with a magnetic stir bar, 1-hexyne (0.0032 g, 3.86×10^{-5} mol) was added and the mixture stirred for 3 h at 140°C . Product **5a** was formed in 90% yield, as determined by NMR spectroscopy.

Synthetic Procedure for 5a, 5b, 5d, 5e, 5g, 5h: $\text{Ni}(\text{acac})_2$ (7.7 mg, 3×10^{-5} mol), the five-membered dichacogenide (**4a** or **4b**; 1×10^{-3} mol), 0.3 mL of toluene, and PMe_2Ph (42 mg, 3×10^{-4} mol) were placed into a PTFE-sealed tube equipped with a magnetic stir bar and the mixture stirred at room temperature until a homogeneous dark-brown solution had formed (ca. 2–3 min). Alkyne (1.2×10^{-3} mol) was then added and the mixture stirred for 4 h at 100°C .

Synthetic Procedure for 5c, 5f, 5i: $\text{Ni}(\text{acac})_2$ (7.7 mg, 3×10^{-5} mol), **4c** (120 mg, 1×10^{-3} mol), 0.5 mL of toluene, and PMe_2Ph (42 mg, 3×10^{-4} mol) were placed into a PTFE-sealed tube equipped with a magnetic stir bar and the mixture stirred at room temperature until a homogeneous dark-brown solution had formed (ca. 2–3 min). The alkyne (3×10^{-3} mol) was then added and the mixture stirred for 10 h at 100°C .

Synthetic Procedure for 5j–5l: $\text{Ni}(\text{acac})_2$ (11.6 mg, 4.5×10^{-5} mol), **4d** (228 mg, 1×10^{-3} mol), 0.3 mL of toluene, and PMe_2Ph (62 mg, 4.5×10^{-4} mol) were placed into a PTFE-sealed tube equipped with a magnetic stir bar and the mixture stirred at room temperature until a homogeneous dark-brown solution had formed (ca. 2–3 min). Alkyne (2×10^{-3} mol) was then added and the mixture stirred for 4 h at 100°C .

Compound Purification and Characterization: After completion of the reaction, the products were purified by dry column flash chromatography on silica.^[36] Dry column flash chromatography has several practical advantages: i) only small amounts of silica are required; ii) quick elution; iii) economy of solvents. However, slightly better yields of isolated products (5–10%) can be achieved by using conventional column chromatography.

Hexanes/dichloromethane (for **5a**, **5b**, **5c**, **5j**, **5k**), hexanes/chloroform (for **5e**), and hexanes/ethyl acetate (for **5d**, **5f**, **5g**, **5i**, **5h**, **5l**) elution gradients were used. Prior to chromatography of products **5g**, **5h**, **5i**, **5l**, the silica was washed with a solution of 5–6 drops of Et_3N in 20 mL of hexanes. Pure products were obtained after drying in vacuo. The products were isolated as colorless or light brown oils and the isolated yields given below were calculated based on the initial amount of **4**.

Methyl 5-(3-Butyl-6,7-dihydro-5H-1,4-dithiepin-5-yl)pentanoate (5a') and Methyl 5-(2-Butyl-6,7-dihydro-5H-1,4-dithiepin-5-yl)pentanoate (5a''): ^1H NMR (500 MHz, CDCl_3): δ = 0.89 (t, J = 14.7 Hz, 3 H), 0.90 (t, J = 14.7 Hz, 3 H), 1.22–1.35 (m, 4 H), 1.38–1.71 (m, 16 H), 1.83–1.94 (m, 2 H), 2.08–2.25 (m, 6 H), 2.32 (t, J = 14.7 Hz, 2 H), 2.33 (t, J = 14.7 Hz, 2 H), 2.65–2.77 (m, 2 H), 3.66 (s, 3 H), 3.67 (s, 3 H), 3.96–4.12 (m, 4 H), 5.73 (s, 1 H), 5.82 (s, 1 H) ppm. $^{13}\text{C}\{^1\text{H}\}$ NMR (126 MHz, CDCl_3): δ = 13.77, 13.79, 21.86, 21.93, 24.66, 24.69, 26.60, 26.64, 30.49, 30.79, 30.88, 30.96, 33.84, 33.86, 34.82, 34.99, 38.28, 38.31, 40.04, 40.05, 40.50, 40.51,

46.22, 46.24, 51.38, 51.39, 136.42, 137.66, 173.87, 173.88 ppm. MS (EI): m/z (%) 302 (95) [M^+]. $C_{15}H_{26}O_2S_2$ (302.50): calcd. C 59.56, H 8.66, S 21.20; found C 59.59, H 8.61, S 20.99, yield 89% (0.252 g).

2-Butyl-6,6-dimethyl-6,7-dihydro-5H-1,4-dithiepine (5b): 1H NMR (500 MHz, $CDCl_3$): δ = 0.89 (t, J = 13.7 Hz, 3 H), 1.12 (s, 6 H), 1.30 (m, 2 H), 1.45 (quint, J = 14.7, J = 15.2 Hz, 2 H), 2.10 (t, J = 15.4 Hz, 2 H), 3.10 (s, 2 H), 3.11 (s, 2 H), 5.65 (s, 1 H) ppm. $^{13}C\{^1H\}$ NMR (126 MHz, $CDCl_3$): δ = 13.85, 21.92, 26.87, 30.92, 35.69, 39.88, 43.46, 43.68, 112.59, 134.55 ppm. MS (EI): m/z (%) 216 (90) [M^+]. $C_{11}H_{20}S_2$ (216.41): calcd. C 61.05, H 9.32, S 29.63; found C 61.17, H 9.36, S 29.27, yield 86% (0.175 g).

2-Butyl-5,6,7,8-tetrahydro-1,4-dithiocine (5c): 1H NMR (500 MHz, $CDCl_3$): δ = 0.91 (t, J = 7.41 Hz, 3 H), 1.32 (m, 2 H), 1.53 (quint, J_1 = 7.33, J_2 = 7.60 Hz, 2 H), 2.05 (m, 4 H), 2.22 (t, J = 7.60 Hz, 2 H), 3.21 (m, 2 H), 3.49 (m, 2 H), 6.17 (s, 1 H) ppm. $^{13}C\{^1H\}$ NMR (126 MHz, $CDCl_3$): δ = 13.78, 22.02, 26.80, 28.72, 31.45, 33.10, 33.73, 41.67, 117.44, 143.99 ppm. MS (EI): m/z (%) 202 (9) [M^+]. $C_{10}H_{18}S_2$ (202.38): calcd. C 59.35, H 8.96, S 31.69; found C 59.31, H 9.06, S 31.37, yield 62% (0.126 g).

Methyl 5-[3-(Methoxymethyl)-6,7-dihydro-5H-1,4-dithiepin-5-yl]pentanoate (5d') and Methyl 5-[2-(Methoxymethyl)-6,7-dihydro-5H-1,4-dithiepin-5-yl]pentanoate (5d''): 1H NMR (500 MHz, $CDCl_3$): δ = 1.39–1.71 (m, 12 H), 1.87–1.98 (m, 2 H), 2.17–2.26 (m, 2 H), 2.32 (m, 4 H), 2.72 (d, J = 14.8 Hz, 1 H), 2.82 (d, J = 14.8 Hz, 1 H), 3.31 (s, 3 H), 3.32 (s, 3 H), 3.67 (s, 3 H), 3.68 (s, 3 H), 3.84 (s, 2 H), 3.86 (s, 2 H), 4.02–4.29 (m, 4 H), 6.03 (s, 1 H), 6.10 (s, 1 H) ppm. $^{13}C\{^1H\}$ NMR (126 MHz, $CDCl_3$): δ = 24.54, 24.56, 26.43, 26.48, 30.06, 30.85, 33.71, 33.72, 34.59, 34.89, 37.77, 37.84, 45.75, 46.56, 51.30, 51.31, 57.30, 57.43, 77.15, 77.45, 118.77, 119.16, 131.51, 132.27, 173.71, 173.73 ppm. MS (EI): m/z (%) 290 (27) [M^+]. $C_{13}H_{22}O_3S_2$ (290.44): calcd. C 53.76, H 7.63, S 22.08; found C 53.98, H 7.85, S 21.92, yield 73% (0.189 g).

2-(Methoxymethyl)-6,6-dimethyl-6,7-dihydro-5H-1,4-dithiepine (5e): 1H NMR (500 MHz, $CDCl_3$): δ = 1.08 (s, 6 H), 3.08 (s, 2 H), 3.10 (s, 2 H), 3.24 (s, 3 H), 3.76 (s, 2 H), 5.89 (s, 1 H) ppm. $^{13}C\{^1H\}$ NMR (126 MHz, $CDCl_3$): δ = 26.77, 35.45, 42.83, 43.77, 57.36, 77.16, 117.62, 130.14 ppm. MS (EI): m/z (%) 204 (73) [M^+]. $C_9H_{16}OS_2$ (204.35): calcd. C 52.90, H 7.89, S 31.38; found C 53.02, H 7.74, S 31.19, yield 91% (0.174 g).

2-(Methoxymethyl)-5,6,7,8-tetrahydro-1,4-dithiocine (5f): 1H NMR (500 MHz, $CDCl_3$): δ = 2.07 (m, 4 H), 3.10 (m, 2 H), 3.33 (s, 3 H), 3.69 (m, 2 H), 3.89 (s, 2 H), 6.67 (s, 1 H) ppm. $^{13}C\{^1H\}$ NMR (126 MHz, $CDCl_3$): δ = 24.85, 30.51, 30.91, 34.76, 57.58, 79.07, 128.52, 129.36 ppm. MS (EI): m/z (%) 190 (39) [M^+]. $C_8H_{14}OS_2$ (190.33): calcd. C 50.48, H 7.41, S 33.69; found C 50.70, H 7.67, S 33.59, yield 59% (0.112 g).

Methyl 5-[3-[(Dimethylamino)methyl]-6,7-dihydro-5H-1,4-dithiepin-5-yl]pentanoate (5g') and Methyl 5-[2-[(Dimethylamino)methyl]-6,7-dihydro-5H-1,4-dithiepin-5-yl]pentanoate (5g''): 1H NMR (500 MHz, $CDCl_3$): δ = 1.38–1.72 (m, 12 H), 1.82–1.96 (m, 2 H), 2.20 (m, 2 H), 2.21 (s, 6 H), 2.22 (s, 6 H), 2.32 (m, 4 H), 2.67–2.86 (m, 4 H), 2.93 (d, J = 12.8 Hz, 1 H), 3.03 (d, J = 12.8 Hz, 1 H), 3.66 (s, 3 H), 3.67 (s, 3 H), 4.00–4.29 (m, 4 H), 5.89 (s, 1 H), 5.98 (s, 1 H) ppm. $^{13}C\{^1H\}$ NMR (126 MHz, $CDCl_3$): δ = 24.38, 24.41, 26.25, 26.32, 30.17, 30.53, 33.52, 33.55, 34.48, 34.71, 37.60, 37.75, 44.57, 44.61, 45.74, 45.81, 51.07, 51.08, 67.97, 68.55, 117.08, 117.22, 132.79, 133.62, 173.45, 173.48 ppm. MS (EI): m/z (%) 303 (10) [M^+]. $C_{14}H_{25}NO_2S_2$ (303.48): calcd. C 55.41, H 8.30, S 21.13; found C 55.52, H 8.37, S 21.03, yield 77% (0.207 g).

N-[(6,6-Dimethyl-6,7-dihydro-5H-1,4-dithiepin-2-yl)methyl]dimethylamine (5h): 1H NMR (500 MHz, $CDCl_3$): δ = 1.13 (s, 6 H), 2.21

(s, 6 H), 2.87 (s, 2 H), 3.14 (s, 2 H), 3.15 (s, 2 H), 5.84 (s, 1 H) ppm. $^{13}C\{^1H\}$ NMR (126 MHz, $CDCl_3$): δ = 26.75, 35.49, 43.17, 43.67, 44.76, 68.18, 116.01, 131.80 ppm. MS (EI): m/z (%) 217 (65) [M^+]. $C_{10}H_{19}NS_2$ (217.39): calcd. C 55.25, H 8.81, N 6.44, S 29.50; found C 55.58, H 8.80, N 6.19, S 29.35, yield 72% (0.141 g).

N,N-Dimethyl(5,6,7,8-tetrahydro-1,4-dithiocin-2-yl)methanamine (5i): 1H NMR (500 MHz, $CDCl_3$): δ = 2.06 (m, 4 H), 2.23 (s, 6 H), 2.95 (s, 2 H), 3.33 (m, 2 H), 3.46 (m, 2 H), 6.45 (s, 1 H) ppm. $^{13}C\{^1H\}$ NMR (126 MHz, $CDCl_3$): δ = 27.07, 28.64, 32.45, 33.64, 45.10, 70.09, 124.23, 135.77 ppm. MS (EI): m/z (%) 203 (9) [M^+]. $C_9H_{17}NS_2$ (203.37): calcd. C 53.15, H 8.43, S 31.53; found C 53.28, H 8.43, S 31.65, yield 74% (0.150 g).

2-Butyl-6,6-dimethyl-6,7-dihydro-5H-1,4-diselenepine (5j): 1H NMR (500 MHz, $CDCl_3$): δ = 0.90 (t, J = 7.4 Hz, 3 H), 1.17 (s, 6 H), 1.31 (m, 2 H), 1.46 (quint, J = 7.4, 2 H), 2.22 (t, J = 7.3 Hz, 2 H), 3.14 (s, 2 H), 3.15 (s, 2 H), 6.22 (s, J = 55 Hz, 1 H) ppm. $^{13}C\{^1H\}$ NMR (126 MHz, $CDCl_3$): δ = 13.84, 21.90, 27.00, 31.32, 35.07, 37.68, 38.59, 42.28, 107.92, 133.07 ppm. MS (EI): m/z (%) 310 (13) [M^+]. $C_{11}H_{20}Se_2$ (310.20): calcd. C 42.59, H 6.50, Se 50.91; found C 42.73, H 6.52, Se 51.04, yield 50% (0.138 g).

2-(Methoxymethyl)-6,6-dimethyl-6,7-dihydro-5H-1,4-diselenepine (5k): 1H NMR (500 MHz, $CDCl_3$): δ = 1.19 (s, 6 H), 3.17 (s, 2 H), 3.21 (s, 2 H), 3.31 (s, 3 H), 3.92 (s, 2 H), 6.53 (s, J = 55 Hz, 1 H) ppm. $^{13}C\{^1H\}$ NMR (126 MHz, $CDCl_3$): δ = 26.90, 35.04, 37.41, 38.30, 57.38, 79.17, 112.55, 128.88 ppm. MS (EI): m/z (%) 298 (32) [M^+]. $C_9H_{16}OSe_2$ (298.14): calcd. C 36.26, H 5.41, Se 52.97; found C 36.27, H 5.57, Se 52.84, yield 64% (0.152 g).

N-[(6,6-Dimethyl-6,7-dihydro-5H-1,4-diselenepin-2-yl)methyl]dimethylamine (5l): 1H NMR (500 MHz, $CDCl_3$): δ = 1.18 (s, 6 H), 2.21 (s, 6 H), 2.98 (s, 2 H), 3.13 (s, 2 H), 3.19 (s, 2 H), 6.41 (s, J = 55 Hz, 1 H) ppm. $^{13}C\{^1H\}$ NMR (126 MHz, $CDCl_3$): δ = 26.88, 34.96, 37.54, 37.88, 44.84, 70.45, 110.57, 131.03 ppm. MS (EI): m/z (%) 311 (57) [M^+]. $C_{10}H_{19}NSe_2$ (311.18): calcd. C 38.60, H 6.15, N 4.50, Se 50.75; found C 38.92, H 6.07, N 4.67, Se 50.75, yield 56% (0.135 g).

X-ray Crystal Structure Determination: Single crystals of **4d** were obtained upon slow evaporation of a solution in hexanes. Single crystals of **5h** and **5i** were crystallized from MeOH solution as their oxalate salts. Data were collected on a Bruker three-circle diffractometer equipped with a SMART APEX II CCD detector and corrected for absorption using the SADABS program.^[37] Data reduction was performed using the APEX2^[38] and SAINTplus^[39] programs (see Table 7 for further details). The structures were solved by direct methods and refined by full-matrix least-squares techniques on F^2 with anisotropic displacement parameters for all the non-H atoms. The amino-H atoms of the cations and hydroxy-H atoms of the anions in **5h** and **5i** were localized in the difference-Fourier syntheses and included in the refinement with fixed positional and isotropic displacement parameters. The other H atoms of all compounds were placed in calculated positions and refined within the riding model with fixed isotropic displacement parameters [$U_{iso}(H)$ = 1.5 $U_{eq}(C)$ for the CH_3 groups and $U_{iso}(H)$ = 1.2 $U_{eq}(C)$ for the other groups]. All calculations were carried out using the SHELXTL program.^[40]

CCDC-683560 (for **4d**), -683561 (for **5h**), and -683562 (for **5i**) contain the supplementary crystallographic data for this paper. These data can be obtained free of charge from The Cambridge Crystallographic Data Centre via www.ccdc.cam.ac.uk/data_request/cif.

Supporting Information (see also the footnote on the first page of this article): Geometric parameters determined from the X-ray studies.

Table 7. Crystal data and structure refinement for **4d**, **5h** and **5i**.

	4d	5h	5i
Empirical formula	C ₅ H ₁₀ Se ₂	C ₁₂ H ₂₁ NO ₄ S ₂	C ₁₁ H ₁₉ NO ₄ S ₂
Formula weight	228.05	307.42	293.39
Temperature [K]	100(2)	100(2)	100(2)
Wavelength [Å]	0.71073	0.71073	0.71073
Crystal system	monoclinic	monoclinic	monoclinic
Space group	<i>P</i> 2 ₁ / <i>c</i>	<i>P</i> 2 ₁ / <i>c</i>	<i>P</i> 2 ₁ / <i>c</i>
Unit cell dimensions [Å, °]	<i>a</i> = 8.5478(5), <i>a</i> = 90 <i>b</i> = 6.2466(4), <i>β</i> = 98.708(1) <i>c</i> = 13.4168(8), <i>γ</i> = 90°	<i>a</i> = 16.9424(17), <i>a</i> = 90 <i>b</i> = 8.3651(8), <i>β</i> = 90.961(2) <i>c</i> = 10.5296(11), <i>γ</i> = 90	<i>a</i> = 16.4871(8), <i>a</i> = 90 <i>b</i> = 8.4608(4), <i>β</i> = 103.145(1) <i>c</i> = 10.4518(5), <i>γ</i> = 90
Volume [Å ³]	708.13(7)	1492.1(3)	1419.76(12)
<i>Z</i>	4	4	4
Density (calculated) [Mg m ⁻³]	2.139	1.368	1.373
Absorption coefficient [mm ⁻¹]	10.328	0.366	0.381
<i>R</i> (000)	432	656	624
Crystal size [mm]	0.20 × 0.20 × 0.06	0.14 × 0.12 × 0.10	0.30 × 0.20 × 0.20
<i>θ</i> range for data collection [°]	4.0–30.14	2.40–28.00	2.54–30.03
Index ranges	–12 ≤ <i>h</i> ≤ 12 –8 ≤ <i>k</i> ≤ 8 –18 ≤ <i>l</i> ≤ 18	–22 ≤ <i>h</i> ≤ 22 –11 ≤ <i>k</i> ≤ 10 –13 ≤ <i>l</i> ≤ 13	–23 ≤ <i>h</i> ≤ 23 –11 ≤ <i>k</i> ≤ 11 –14 ≤ <i>l</i> ≤ 14
Reflections collected	8789	15662	17835
Independent reflections	2047 [<i>R</i> (int) = 0.0366]	3528 [<i>R</i> (int) = 0.0281]	4099 [<i>R</i> (int) = 0.0296]
Completeness to <i>θ</i> = 30.14° [%]	98.2	98.3	98.8
Absorption correction	semi-empirical from equivalents	semi-empirical from equivalents	semi-empirical from equivalents
Max., min. transmission	0.536, 0.142	0.960, 0.951	0.928, 0.894
Refinement method	full-matrix least-squares on <i>F</i> ²	full-matrix least-squares on <i>F</i> ²	full-matrix least-squares on <i>F</i> ²
Data/restraints/parameters	2047/0/66	3528/0/176	4099/0/165
Goodness-of-fit on <i>F</i> ²	1.014	1.002	1.003
Final <i>R</i> indices	<i>R</i> ₁ = 0.0213, <i>wR</i> ₂ = 0.0489	<i>R</i> ₁ = 0.0388, <i>wR</i> ₂ = 0.0953	<i>R</i> ₁ = 0.0308, <i>wR</i> ₂ = 0.0775
[for 1805 refl. with <i>I</i> > 2σ(<i>I</i>)]			
<i>R</i> indices (all data)	<i>R</i> ₁ = 0.0265, <i>wR</i> ₂ = 0.0511	<i>R</i> ₁ = 0.0466, <i>wR</i> ₂ = 0.1019	<i>R</i> ₁ = 0.0364, <i>wR</i> ₂ = 0.0814
Largest diff. peak and hole [e Å ⁻³]	0.602 and –0.594	0.662 and –0.347	0.430 and –0.540

Acknowledgments

The research was supported by the Russian Foundation for Basic Research (project no. 07-03-00851), a Research grant of the President of Russia (MD-4094.2007.3) and Program No. 1 of the Division of Chemistry and Material Sciences of RAS.

- [1] a) Selected representative articles: L. D. Pachon, G. Rothenberg, *Appl. Organomet. Chem.* **2008**, *22*, 288; b) M. B. Thathagar, J. E. ten Elshof, G. Rothenberg, *Angew. Chem. Int. Ed.* **2006**, *45*, 2886; *Angew. Chem.* **2006**, *118*, 2952; c) D. Astruc, *Inorg. Chem.* **2007**, *46*, 1884; d) A. K. Diallo, C. Ornelas, L. Salmon, J. R. Aranzaes, D. Astruc, *Angew. Chem. Int. Ed.* **2007**, *46*, 8644; *Angew. Chem.* **2007**, *119*, 8798; e) K. Köhler, R. G. Heidenreich, J. G. E. Krauter, J. Pietsch, *Chem. Eur. J.* **2002**, *8*, 622; f) R. G. Heidenreich, E. G. E. Krauter, J. Pietsch, K. Köhler, *J. Mol. Catal. A* **2002**, *182*, 499; g) N. T. S. Phan, M. van Der Sluys, C. W. Jones, *Adv. Synth. Catal.* **2006**, *348*, 609; h) F. Y. Zhao, M. Shirai, Y. Ikushima, M. Arai, *J. Mol. Catal. A* **2002**, *180*, 211; i) A. R. Tao, S. Habas, P. D. Yang, *Small* **2008**, *4*, 310; j) F. Shi, M. K. Tse, M.-M. Pohl, A. Bruckner, S. Zhang, M. Beller, *Angew. Chem. Int. Ed.* **2007**, *46*, 8866; *Angew. Chem.* **2007**, *119*, 9022; k) C. M. Hagen, L. Vieille-Petit, G. Laurenczy, G. Süss-Fink, R. G. Finke, *Organometallics* **2005**, *24*, 1819; l) S. P. Andrews, A. F. Stepan, H. Tanaka, S. V. Ley, M. D. Smith, *Adv. Synth. Catal.* **2005**, *347*, 647; m) W. K. Cho, J. K. Lee, S. M. Kang, Y. S. Chi, H.-S. Lee, I. S. Choi, *Chem. Eur. J.* **2007**, *13*, 6351.
- [2] a) V. P. Ananikov, N. V. Orlov, I. P. Beletskaya, V. N. Khrustalev, M. Yu. Antipin, T. V. Timofeeva, *J. Am. Chem. Soc.* **2007**, *129*, 7252; b) V. P. Ananikov, N. V. Orlov, I. P. Beletskaya, *Organometallics* **2007**, *26*, 740; c) V. P. Ananikov, N. V. Orlov, I. P. Beletskaya, *Organometallics* **2006**, *25*, 1970.
- [3] a) I. P. Beletskaya, V. P. Ananikov, *Eur. J. Org. Chem.* **2007**, 3431; b) I. P. Beletskaya, V. P. Ananikov, *Pure Appl. Chem.* **2007**, *79*, 1041.
- [4] The non-catalytic addition of 1,2-dithiolanes to alkynes suffers from polymerization of the cyclic disulfides. This reaction is possible only for polymerization-resistant substrates (for E = Se the reaction is unknown), see: a) M. Tazaki, M. Kumakura, S. Nagahama, M. Takagi, *J. Chem. Soc., Chem. Commun.* **1995**, 1763; b) D. V. Demchuk, G. I. Nikishin, *Russ. Chem. Bull. Int. Ed.* **1997**, *46*, 199.
- [5] For other studies on related subjects, see: a) A. Ogawa, *J. Organomet. Chem.* **2000**, *611*, 463; b) H. Kuniyasu, A. Ogawa, S. Miyazaki, I. Ryu, N. Kambe, N. Sonoda, *J. Am. Chem. Soc.* **1991**, *113*, 9796.
- [6] For addition reactions with this and other ligands, see: a) V. P. Ananikov, M. A. Kabeshov, I. P. Beletskaya, V. N. Khrustalev, M. Yu. Antipin, *Organometallics* **2005**, *24*, 1275; b) V. P. Ananikov, K. A. Gayduk, I. P. Beletskaya, V. N. Khrustalev, M. Yu. Antipin, *Chem. Eur. J.* **2008**, *14*, 2420.
- [7] For homogeneous systems, it is well known that an excess of ligand blocks the catalyst's binding sites and does not allow substrate molecules to coordinate. For reviews on this topic, see: a) M. Beller, J. Seayad, A. Tillack, H. Jiao, *Angew. Chem. Int. Ed.* **2004**, *43*, 3368; b) M. Sugimoto, Y. Ito, *J. Organomet. Chem.* **2003**, *685*, 218; c) M. Sugimoto, Y. Ito, *J. Organomet. Chem.* **2003**, *680*, 43; d) T. Kondo, T. Mitsudo, *Chem. Rev.* **2000**, *100*, 3205; e) I. Beletskaya, C. Moberg, *Chem. Rev.* **2006**, *106*, 2320; f) *Catalytic Heterofunctionalization* (Eds.: A. Togni, H. Grützmaier), Wiley-VCH, Weinheim, **2001**; g) I. Beletskaya, C. Moberg, *Chem. Rev.* **1999**, *99*, 3435.
- [8] V. P. Ananikov, I. P. Beletskaya, G. G. Aleksandrov, I. L. Eremenko, *Organometallics* **2003**, *22*, 1414.
- [9] M. S. Hannu, R. Oilunkaniemi, R. S. Laitinen, M. Ahlgen, *Inorg. Chem. Commun.* **2000**, *3*, 397.

- [10] R. Oilunkaniemi, R. S. Laitinen, M. Ahlgren, *J. Organomet. Chem.* **1999**, 587, 200.
- [11] V. P. Ananikov, I. P. Beletskaya, *Org. Biomol. Chem.* **2004**, 2, 284.
- [12] I. Nakanishi, S. Tanaka, K. Matsumoto, S. Ooi, *Acta Crystallogr., Sect. C* **1994**, 50, 58.
- [13] R. Oilunkaniemi, R. S. Laitinen, M. Ahlgren, *J. Organomet. Chem.* **2001**, 623, 168.
- [14] D. Shimizu, N. Takeda, N. Tokitoh, *Chem. Commun.* **2006**, 177.
- [15] M. S. Hannu-Kuure, A. Wagner, T. Bajorek, R. Oilunkaniemi, R. S. Laitinen, M. Ahlgren, *Main Group Chem.* **2005**, 4, 49.
- [16] S. Berger, S. Braun, H. O. Kalinowski, *NMR spectroscopy of the non-metallic elements*, Wiley, Chichester, **1997**.
- [17] V. P. Ananikov, N. V. Orlov, I. P. Beletskaya, *Russ. Chem. Bull. Int. Ed.* **2005**, 54, 576.
- [18] *Transition Metal Nuclear Magnetic Resonance* (Ed.: P. S. Pregosin), Elsevier, Amsterdam, Oxford, New York, Tokyo, **1991**.
- [19] *Cambridge Structural Database*, release 2008, Cambridge, **2008**.
- [20] a) E. W. Abel, P. K. Mittal, K. G. Orrell, V. Sik, T. S. Cameron, *J. Chem. Soc., Chem. Commun.* **1984**, 1312; b) E. W. Abel, P. K. Mittal, K. G. Orrell, H. Dawes, M. B. Hursthouse, *Polyhedron* **1987**, 6, 2073.
- [21] H. Bock, U. Stein, A. Semkow, *Chem. Ber.* **1980**, 113, 3208.
- [22] L. Teuber, *Sulfur Rep.* **1990**, 9, 257.
- [23] a) A. E. Pullen, C. Faulmann, P. Cassoux, *Eur. J. Inorg. Chem.* **1999**, 269; b) C. W. Ong, C. Y. Yu, *Tetrahedron* **2003**, 59, 9677.
- [24] T. Ukai, H. Kawazura, Y. Ishii, J. J. Bonnet, J. A. Ibers, *J. Organomet. Chem.* **1974**, 65, 253.
- [25] T. N. Mitchell, A. Amamria, H. Killing, D. Rutschow, *J. Organomet. Chem.* **1986**, 304, 257.
- [26] See, for example: a) J. Houk, G. M. Whitesides, *Tetrahedron* **1989**, 45, 91; b) L. Teuber, C. Christophersen, *Acta Chem. Scand. B* **1988**, 42, 629; c) M. H. Ali, M. McDermott, *Tetrahedron Lett.* **2002**, 43, 6271.
- [27] P. Dhar, N. Chidambaram, S. Chandrasekaran, *J. Org. Chem.* **1992**, 57, 1699.
- [28] Synthesis of **4d**: L. Syper, J. Mlochowski, *Synthesis* **1984**, 5, 439.
- [29] I. C. Gunsalus, L. S. Barton, W. Gruber, *J. Am. Chem. Soc.* **1956**, 78, 1763.
- [30] F. Arndt, *Organic Syntheses*, **1943**, Coll. Vol. 2, 165; **1935**, Vol. 15, 3. <http://orgsyn.org/orgsyn/prep.asp?prep=cv2p0165>.
- [31] S. P. Chavan, K. Shivsankar, K. Pasupathy, *Synthesis* **2005**, 1297.
- [32] G. M. Whitesides, J. D. Roberts, *J. Am. Chem. Soc.* **1965**, 87, 4878.
- [33] E. W. Abel, P. K. Mittal, K. G. Orrell, V. Sik, *J. Chem. Soc., Dalton Trans.* **1985**, 1569.
- [34] S. W. Bass, S. A. Evans, *J. Org. Chem.* **1980**, 45, 710.
- [35] P. Salama, C. Bernard, *Tetrahedron Lett.* **1995**, 36, 5711.
- [36] a) D. S. Pedersen, C. Rosenbohm, *Synthesis* **2001**, 2431; b) L. M. Harwood, *Aldrichimica Acta* **1985**, 18, 25.
- [37] G. M. Sheldrick, SADABS, v. 2.03, *Bruker/Siemens Area Detector Absorption Correction Program*, Bruker AXS, Madison, Wisconsin, USA, **2003**.
- [38] Bruker AXS, APEX2 software package, v. 1.27, Bruker Molecular Analysis Research Tool, Bruker AXS, Madison, Wisconsin, USA, **2005**.
- [39] Bruker AXS, SAINTPlus for NT, v. 6.2, Data Reduction and Correction Program, Bruker AXS, Madison, Wisconsin, USA, **2001**.
- [40] G. M. Sheldrick, SHELXTL for NT, v. 6.12, Structure Determination Software Suite, Bruker AXS, Madison, Wisconsin, USA, **2001**.

Received: October 7, 2008

Published Online: January 23, 2009